Microwave and magnetotransport properties of RuSr2RCu2O8 (R=Eu,Gd) doped with Sn

Požek, Miroslav; Kupčić, Ivan; Dulčić, Antonije; Hamzić, Amir; Paar, Dalibor; Basletić, Mario; Tafra, Emil; Williams, G. V. M.

Source / Izvornik: **Physical review B: Condensed matter and materials physics, 2008, 77**

Journal article, Published version
Rad u časopisu, Objavljena verzija rada (izdavačev PDF)

https://doi.org/10.1103/PhysRevB.77.214514

Permanent link / Trajna poveznica: https://urn.nsk.hr/urn:nbn:hr:217:156426

Microwave and magnetotransport properties of $RuSr_2RCu_2O_8$ (R=Eu,Gd) doped with Sn

M. Požek, I. Kupčić, A. Dulčić, A. Hamzić, D. Paar, M. Basletić, and E. Tafra
Department of Physics, Faculty of Science, University of Zagreb, P.O. Box 331, HR-10002 Zagreb, Croatia

G. V. M. Williams
Industrial Research Limited, P.O. Box 31310, Lower Hutt, New Zealand

(Received 10 December 2007; revised manuscript received 21 April 2008; published 17 June 2008)

$Ru_{1-x}Sn_xSr_2EuCu_2O_8$ and $Ru_{1-x}Sn_xSr_2GdCu_2O_8$ have been comprehensively studied by microwave and dc resistivity and magnetoresistivity and by the Hall measurements. The ruthenium magnetic ordering temperature T_m is considerably reduced with increasing Sn content. However, doping with Sn leads to only slight reduction of the superconducting critical temperature T_c accompanied with the increase in the upper critical field B_{c2}, indicating an increased disorder in the system and a reduced scattering length of the conducting holes in CuO_2 layers. In spite of the increased scattering rate, the normal state resistivity and the Hall resistivity are reduced with respect to the pure compound, due to the increased number of itinerant holes in CuO_2 layers, which represent the main conductivity channel. Most of the electrons in RuO_2 layers are presumably localized, but the observed negative magnetoresistance and the extraordinary Hall effect lead to the conclusion that there exists a small number of itinerant electrons in RuO_2 layers that exhibit colossal magnetoresistance.

DOI: 10.1103/PhysRevB.77.214514 PACS number(s): 74.70.Pq, 74.25.Fy, 74.25.Ha, 75.47.Gk

I. INTRODUCTION

Despite the intensive investigation of ruthenate-cuprates in the last ten years, a lot of questions about the nature of magnetic order and superconductivity, in particular their coexistence, are still unanswered.[1] It is well established that in $RuSr_2RCu_2O_8$ (Ru1212R,R=Eu,Gd,Y) compounds the magnetic ordering of ruthenium sublattice occurs at about 130 K. The ordering is predominantly antiferromagnetic (AFM) with an easy axis perpendicular to the layers and with a weak ferromagnetic (FM) component parallel to the layers.

While both RuO_2 and CuO_2 layers may participate in the normal-state conductivity, the superconducting (SC) properties of Ru1212R compounds are associated only with the charge carriers in the CuO_2 planes, and are, thus, strongly dependent on the concentration of these carriers. The related superconducting critical temperature T_c ranges between 15 K and 50 K, depending on the sample composition and/or sample preparation conditions. According to the thermopower and Hall coefficient measurements, pure Ru1212R samples are expected to be intrinsically underdoped, with the effective hole concentration in the CuO_2 planes nearly equal to $p \approx 0.07$.[2]

In high-T_c superconductors, SC properties are strongly dependent on the effective hole concentration p in the CuO_2 planes. In the optimally doped systems, the effective hole concentration is estimated to be $p \approx 0.16$ holes/Cu. In this respect, in recent years there has been a lot of experimental effort to adjust the number of charge carriers in the CuO_2 planes in Ru1212R samples using different substitutional impurities. The largest changes in T_c are found when Ru is partially replaced by Cu ($T_c \approx 75$ K for 40% of Ru replaced by Cu).[3] In several studies ruthenium was replaced by Nb^{5+}, $V^{4+,5+}$ Sn^{4+}, Ti^{4+}, and Rh^{3+} (Ref. 2 and Refs. 4–11). Substitutions have also been made for other ions. For example, trivalent gadolinium was replaced by Ca^{2+} and Ce^{4+} (Ref. 12) or by isovalent Y and Dy.[2] Finally, divalent strontium was replaced by La^{3+} and Na^+.[5,6] If the substitutional impurity lowers the total number of holes (La^{3+} for Sr^{2+}, Ce^{4+} for Gd^{3+}, and Nb^{5+} for Ru^{4+}), T_c is strongly depressed, indicating that p is reduced well below 0.07. However, in the cases when valence counting of impurities would suggest a strong increase in p (Na^+ for Sr^{2+} and Sn^{4+} for Ru^{5+}), no substantial increase in T_c was experimentally observed, contrary to the observation in common high-T_c systems with substitutional impurities. This is rather similar to the observation in the underdoped $YBa_2Cu_3O_{7-x}$ compounds where $T_c \approx 60$ K is nearly constant in a wide range of x. The increase in T_c was only observed in Ca^{2+} substitution for Gd^{3+},[12] but it can be attributed to the formation of $Ru_{1-x}Sr_2GdCu_{2+x}O_8$ phase. The magnetic ordering is, however, strongly influenced by the substitutions in all of the mentioned doping studies.

There is still an open debate whether RuO_2 layers are conducting or not. The magnetization[13] and nuclear quadrupole resonance (NQR) (Refs. 14 and 15) results suggest that most of the electrons are localized resulting in Ru^{4+} ions while magnetoresistivity and Hall measurements[2,16] suggest the existence of conductivity in magnetically ordered RuO_2 layers. We shall deal with this question in our doping study, where the number of charge carriers is modified by the replacement of Ru ions with Sn. In this paper a comprehensive microwave study on several Ru1212Eu and Ru1212Gd samples doped with Sn is reported. One of the samples ($Ru_{0.8}Sn_{0.2}Sr_2GdCu_2O_8$) is also characterized by transport, magnetoresistance and Hall measurements, and the results are compared with our previous measurements.[16,17]

In this context, it is important to point out the controversy related to the role of the Sn substitution on Ru sites in Ru1212Gd samples. McLaughlin *et al.*[4,7] and Hassen and Mandal[6] reported, respectively, the increase and decrease in T_c with doping. It is possible that this controversy reflects different ways to experimentally determine T_c, or might be related to different methods of sample preparation. Moreover, we shall revise the observation in the Hall study (Fig. 2 in Ref. 2) in which the increase in the Hall coefficient with increased Sn content was reported.

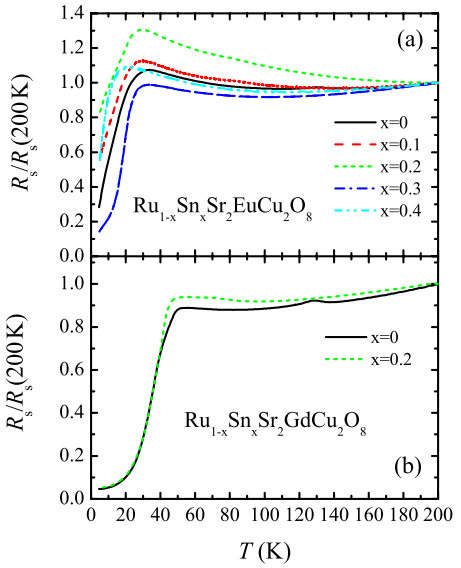

FIG. 1. (Color online) Temperature dependence of the normalized surface resistance of (a) $Ru_{1-x}Sn_xSr_2EuCu_2O_8$ and (b) $Ru_{1-x}Sn_xSr_2GdCu_2O_8$ for various Sn concentrations x.

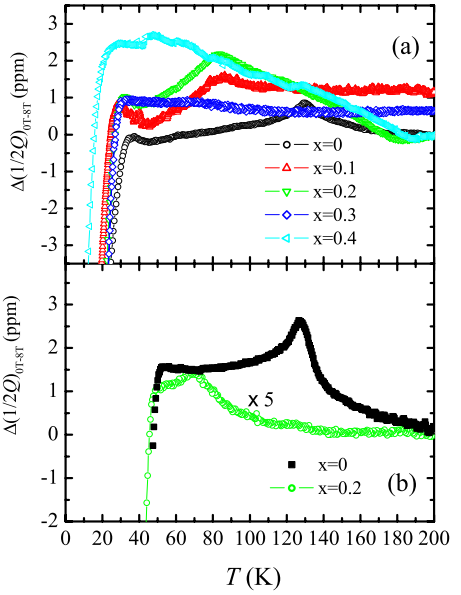

FIG. 2. (Color online) Differences in the microwave resistance in zero field and $B=8$ T of (a) $Ru_{1-x}Sn_xSr_2EuCu_2O_8$ and (b) $Ru_{1-x}Sn_xSr_2GdCu_2O_8$ for various x. (A considerably smaller signal of Sn-doped sample with respect to the pure Gd-based sample is mainly due to the smaller geometry of the former.)

II. EXPERIMENTAL DETAILS

$Ru_{1-x}Sn_xSr_2RCu_2O_8$ (R=Eu or Gd) polycrystalline samples were prepared by solid state synthesis, as described elsewhere.[5] An elliptical ${}_eTE_{111}$ copper cavity operating at 9.3 GHz was used for the microwave measurements. The sample was placed in the center of the cavity on a sapphire holder. At this position the microwave electric field has its maximum. External dc magnetic field perpendicular to the microwave electric field was varied from zero up to 8 T. The temperature of the sample could be varied from liquid helium to room temperature. The measured quantity was $1/2Q$, the total losses of the cavity loaded by the sample. It is simply related to the surface resistance of the material R_s which comprises both nonresonant resistance and resonant spin contributions. The details of the detection scheme are given elsewhere.[18]

Resistivity, magnetoresistance, and Hall effect measurements were carried out in the standard six-contact configuration using the rotational sample holder and the conventional ac technique (22 Hz, 1 mA), in magnetic fields up to 8 T. Temperature sweeps for the resistivity measurements were performed with carbon-glass and platinum thermometers, while magnetic field dependent sweeps were done at constant temperatures which were controlled with a capacitance thermometer.

III. RESULTS AND ANALYSES

A. Microwave properties

The temperature dependence of the microwave surface resistance of various Ru1212Eu (Sn doping x=0, 0.1, 0.2, 0.3, and 0.4) and Ru1212Gd (x=0, 0.2) compounds is shown in Figs. 1(a) and 1(b), respectively. The data are normalized at T=200 K, for comparison. We found that, for the samples of similar geometry, the absolute level of the normal-state absorption in the Eu-based samples was systematically higher than the absorption in the Gd-based samples. Moreover, the surface resistance of the Eu-based samples shows more pronounced rise as the temperature decreases toward the SC ordering temperature T_c than it is the case in Gd-based samples. The related crossover to the SC state occurs at lower temperatures. The SC crossover temperature region is rather broad in these data, resulting in a rather uncertain estimation of T_c. This problem can be easily solved by plotting the difference between the microwave absorption in zero field and in B=8 T (Fig. 2). Both the magnetic and SC transitions can be detected here with a much better accuracy than in Fig. 1.

The magnetic ordering temperature T_m of the Ru lattice corresponds with small peaks clearly seen in Fig. 2. The dependence of T_m on the Sn content x is shown in Figs. 3(a) and 3(b). T_m is strongly suppressed with increasing x in both the Gd- and Eu-based samples (the magnetic critical temperature T_m is reduced nearly by a factor of 2 for $\Delta x \approx 0.2$).

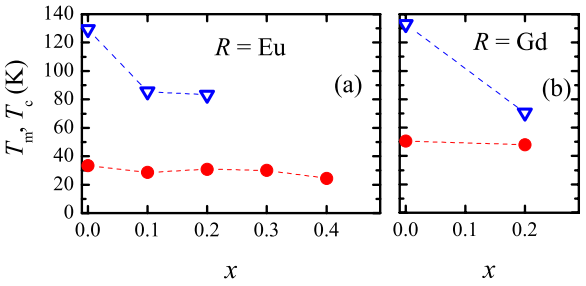

FIG. 3. (Color online) Dependence of T_m (open triangles) and T_c (full circles) on x in $Ru_{1-x}Sn_xSr_2MCu_2O_8$, for (a) R=Eu and (b) R=Gd.

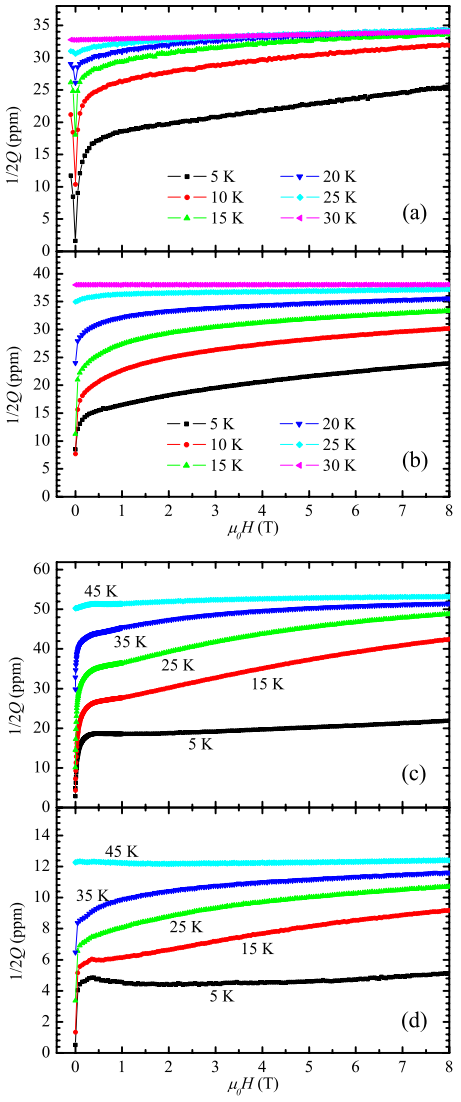

FIG. 4. (Color online) Magnetic field dependence of the microwave absorption for (a) $RuSr_2EuCu_2O_8$, (b) $Ru_{0.7}Sn_{0.3}Sr_2EuCu_2O_8$, (c) $RuSr_2GdCu_2O_8$, and (d) $Ru_{0.8}Sn_{0.2}Sr_2GdCu_2O_8$ measured at various temperatures.

This suppression seems to be a consequence of the reduced content of the Ru magnetic ions (dilution of the magnetic lattice) and the increased disorder in the Ru lattice. Similar decrease in T_m is found in the samples in which Ru is replaced by nonmagnetic Nb^{5+} ions[2] [$\Delta T_m \approx 30$ K for $\Delta x \approx 0.2$ (Ref. 4)].

T_c is here defined by a sudden drop in the difference of the microwave absorption in zero field and in $B=8$ T. Namely, close to T_c, superconductivity develops first in the grains. Since the upper critical fields at those temperatures are lower than 8 T, the applied magnetic field destroys this superconductivity and brings about an increase in the microwave resistance. Hence, the drop in Fig. 2 indicates the onset of the SC state in the grains and can be associated with the intrinsic value of T_c. The whole sample is expected to become superconducting at much lower temperatures where the 3D network of intergranular Josephson junctions is established. T_c is clearly seen in Fig. 2 for all the samples, and its

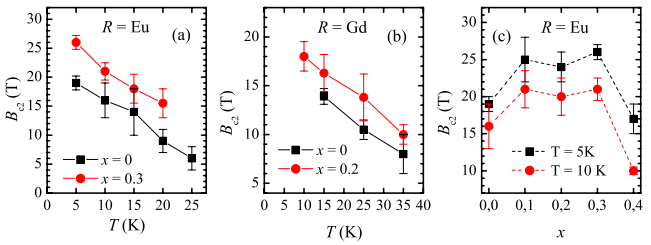

FIG. 5. (Color online) (a) Dependence of the upper critical field B_{c2} on temperature in $Ru_{1-x}Sn_xSr_2EuCu_2O_8$, for $x=0$ (squares) and $x=0.3$ (circles). (b) Dependence of B_{c2} on temperature in $Ru_{1-x}Sn_xSr_2GdCu_2O_8$, for $x=0$ (squares) and $x=0.2$ (circles). (c) Dependence of B_{c2} on x in $Ru_{1-x}Sn_xSr_2EuCu_2O_8$ at $T=5$ K (squares) and $T=10$ K (circles).

dependence on x is further shown in Fig. 3. It is clear that the influence of Sn doping on T_c is not nearly as dramatic as the influence on T_m. In the Gd-based samples, for example, the replacement of 20% of Ru by Sn does not appreciably change T_c. In the Eu-based samples, on the other hand, a slight reduction in T_c with increasing x is observed, but it is negligible in comparison to the related change in T_m.

The SC state is further analyzed by measuring the magnetic-field dependence of the microwave absorption. The results taken at different temperatures are shown in Fig. 4 for two undoped samples and two Sn-doped samples. At lower fields (below 0.5 T), the microwave absorption is strongly field-dependent due to the intergranular superconductivity dominated by the 3D Josephson network. At higher fields, all the Josephson junctions are driven to the normal state, and superconductivity is localized only in the grains. The microwave absorption grows slowly in this field range as the number of vortices increases, and it is expected to reach the normal-state absorption at the upper critical field B_{c2}. The microwave magnetoresistance is therefore a useful tool for the estimation of upper critical fields. If one assumes that the depinning frequency is lower than the driving microwave frequency, it suffices to extrapolate the microwave absorption curves to the normal-state values and determine B_{c2}. However, this simple determination of B_{c2} is not possible in cases where the depinning frequency is comparable to the driving frequency. Then, one has to take into account also the frequency shift. The details of the complete procedure are explained in Ref. 19. The shape of the low-temperature microwave magnetoresistance curves of the Gd-based samples [$T=5$ K curves in Figs. 4(c) and 4(d)] points at the regime where the two frequencies are comparable to each other. At higher temperatures, on the other hand, the driving microwave frequency seems to be larger than the depinning frequency allowing the direct estimation of the upper critical fields. In the Eu-based samples, the depinning frequency seems to be low enough even at low temperatures, so that the upper critical fields can be simply determined in the complete temperature region of Figs. 4(a) and 4(b).

The upper critical fields B_{c2} estimated from the curves in Fig. 4 (and similar curves for other samples not shown here) are plotted in Fig. 5. The comparison of B_{c2} estimated in two Eu-based samples, $x=0$ and 0.3, is shown in Fig. 5(a). The analogous comparison of B_{c2} in the Gd-based samples with

$x=0$ and 0.2 is given in Fig. 5(b). From these figures one can see that the upper critical fields in the Gd-based samples are lower than in the Eu-based samples, and, in both cases, the upper critical fields are higher in the doped samples than in the undoped samples. Bearing in mind that higher B_{c2} means lower Ginzburg–Landau coherence length, which, in turn, depends on the electron mean free path, one concludes that the disorder in the undoped Eu-based samples is higher than in the undoped Gd-based samples, and that the Sn doping introduces an additional disorder in both systems. The low-temperature ($T=5$ K and 10 K) dependence of the upper critical field on the Sn concentration x in the Eu-based samples is also shown [Fig. 5(c)]. From Fig. 5(c), we can see that the upper critical field increases with x for low to moderate concentrations, while for the highest concentration ($x=0.4$) B_{c2} is suppressed. The drop of B_{c2} in the $x=0.4$ sample is related to the drop of T_c in Fig. 3(a).

B. Magnetotransport properties

In order to clarify the role of the disorder introduced by Sn doping, we extend the experimental study and analysis to transport coefficients. We have chosen the doped sample $Ru_{0.8}Sn_{0.2}Sr_2GdCu_2O_8$ which exhibits a sharp SC onset in Fig. 2(b), and measured its resistivity, magnetoresistivity, and Hall resistivity.

Figure 6(a) shows the resistivity measured in zero magnetic field and in $\mu_0 H=8$ T. In both cases, the resistivity at 200 K is 9.5 mΩ cm, which is much lower than 15.5 mΩ cm of the undoped sample.[16] In zero field, one observes a relatively broad SC transition characterized by the change in the magnitude from 90% to 10% within the temperature interval $\Delta T=8$ K. Such temperature dependence of the resisitivity in the vicinity of T_c is usually attributed to the spontaneous vortex phase. The temperature interval characterizing the SC transition in the 8 T resistivity data is much broader than that of the zero-field data, and the zero resistance occurs only at 10 K, indicating that the pinning above 10 K is not strong enough to suppress the vortex motion, even for dc driving currents. The absence of strong pinning forces above 10 K justifies the estimation of B_{c2} from the magnetic-field dependence of the microwave absorption given above [Fig. 4(d)].

The onset of superconductivity in the grains is better seen if the resistivity in 8 T is subtracted from the zero-field resistivity, as shown in Fig. 6(b). The subtraction also reveals the existence of a broad maximum at the magnetic ordering temperature $T\approx T_m\approx 75$ K. This peak can be further analyzed using magnetic field dependent resistivity measurements. The relative transversal magnetoresistivity $[\rho(H,T)-\rho(0,T)]/\rho(0,T)$ is shown in Fig. 7 in a large temperature range from 140 K down to the superconducting transition. The curves are grouped in five subsets according to temperature intervals in Fig. 6(b) labeled by (a), (b), (c), (d), and (e), exhibiting several qualitatively different physical situations.

At temperatures well above T_m [Fig. 7(a)], the magnetoresistivity is characterized by the negative quadratic-in-field behavior similar to the magnetic-field dependence observed in dilute alloys containing uncorrelated magnetic

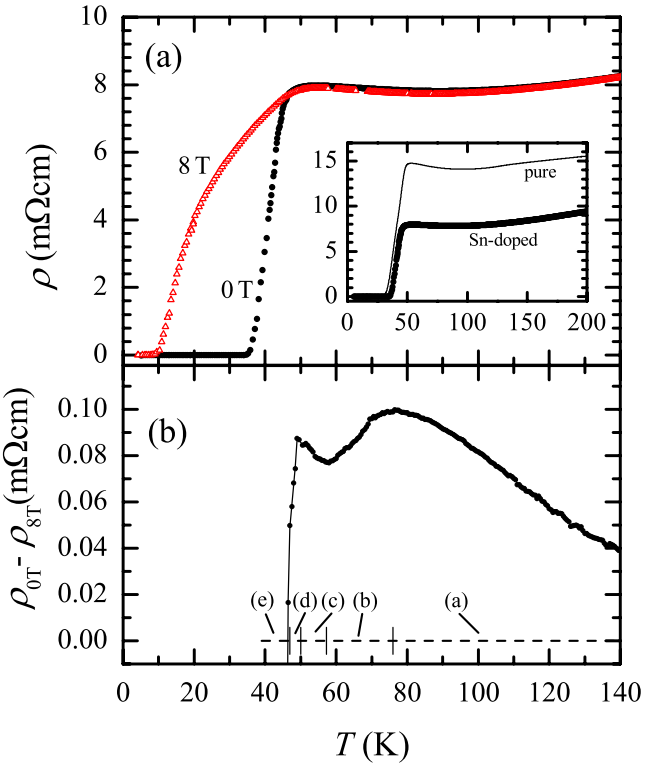

FIG. 6. (Color online) (a) Resistivity of $Ru_{0.8}Sn_{0.2}Sr_2GdCu_2O_8$ measured in zero field (black line) and in $B=8$ T (red line). The inset shows the comparison of resistivity with the resistivity of the undoped sample (thin line) (Ref. 16) (b) Difference between the zero-field and 8 T resistivities. The five temperature intervals labeled by (a), (b), (c), (d), and (e) correspond to subsets of MR curves in Fig. 7.

impurities.[20] With decreasing temperature the correlations between magnetic Ru ions start to play an important role and the quadratic-in-field magnetoresistance transforms into the linear-in-field behavior. The same trend can also be seen for temperatures below T_m [Fig. 7(b)], but not too close to T_c. Not surprisingly, the same linear-in-field behavior was already observed in undoped and in La-doped samples in the vicinity of T_m.[16,17] Just below T_m, superposed to the negative linear magnetoresistivity, a small positive component develops at low fields, which is related to the AFM ordering of the Ru lattice. The same positive contribution is also observed in the longitudinal configuration (i.e., $\mathbf{H}\|\mathbf{I}$). Finally, it should be noticed that the negative magnetoresistivity of Figs. 7(a) and 7(b) does not show any sign of saturation up to $\mu_0 H=8$ T.

Figures 7(c) and 7(d) reveal a relatively complicated behavior of the magnetoresistivity at temperatures between 57 and 47 K. The positive AFM contribution decreases rapidly and vanishes below 53 K. Below 49 K one observes positive contribution, presumably related to the SC fluctuations. The resulting magnetoresistivity, which is the sum of the positive SC and negative FM contribution, yields a local minimum. Finally, below $T=47$ K, the positive contribution to the magnetoresistivity related to the SC ordering of the conducting layers starts to dominate. The sharp increase in the magnitude of the relative magnetoresistivity in this temperature

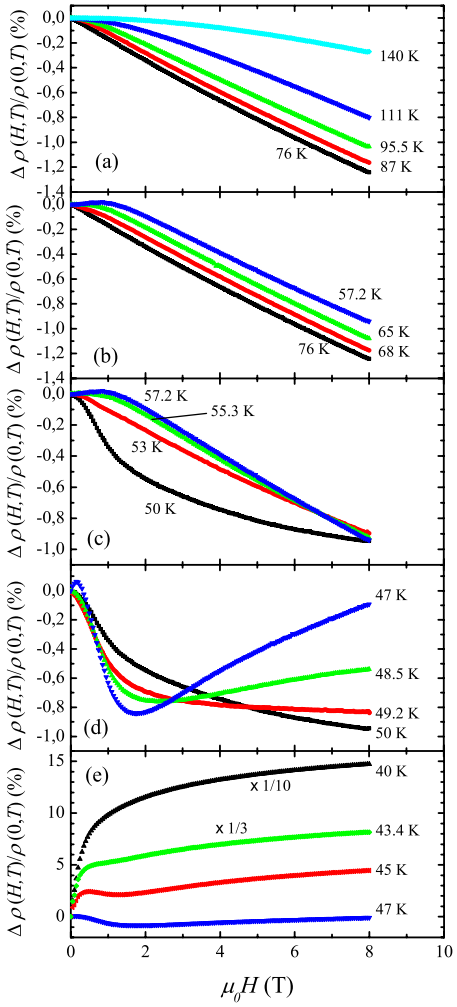

FIG. 7. (Color online) Magnetoresistance of $Ru_{0.8}Sn_{0.2}Sr_2GdCu_2O_8$ in various temperature ranges. The values at 43.4 K and 40 K in (e) are divided by factors of 3 and 10, respectively.

region, shown in Fig. 7(e), reflects the sharp decrease in $\rho(0,T)$ in Fig. 6(a).

C. Hall resistance

So far we have established two seemingly opposed observations: the resisitivity of the Sn-doped sample is lowered with respect to the pure compound, while the electron relaxation rates (proportional to the resisitivity) increase with the Sn concentration x (as estimated from the x dependence of B_{c2}). This controversy could have been trivially explained if the intergranular conductivity in the pure sample was much lower than in the Sn-doped sample. However, this explanation is not very likely for three reasons: (i) The samples were prepared under the same conditions. (ii) From the microwave measurements in Fig. 4, one can see that in both samples one third of the absorption occurs between grains, indicating that the intergranular structure in both samples is similar. (iii) If there were differences in the intergranular composition of the two samples, one would expect a larger amount of spurious phases in the Sn-doped sample than in the pure one.[21] In

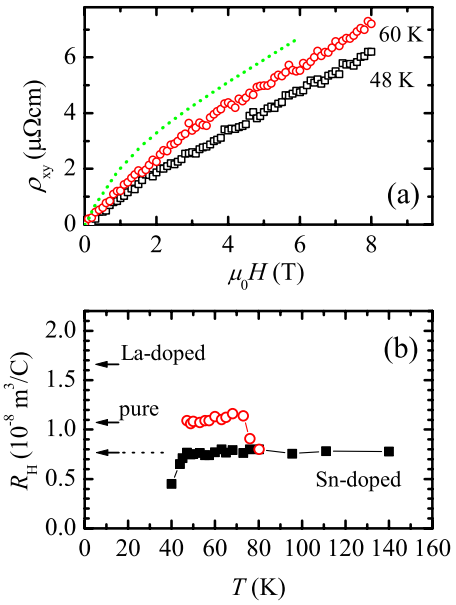

FIG. 8. (Color online) (a) Magnetic field dependence of the Hall resistivity in $Ru_{0.8}Sn_{0.2}Sr_2GdCu_2O_8$ at $T=60$ K (circles) and $T=48$ K (squares). The Hall resistivity of the undoped $RuSr_2GdCu_2O_8$ at $T=124$ K is shown by the dotted line for comparison (Ref. 16). (b) Temperature dependence of the low- (open circles) and high-field (full squares) Hall coefficients of $Ru_{0.8}Sn_{0.2}Sr_2GdCu_2O_8$. The averaged high-field Hall coefficients of the pure $RuSr_2GdCu_2O_8$ and the La-doped $RuSr_{1.9}La_{0.1}GdCu_2O_8$ are indicated by the arrows for comparison.

order to resolve the above controversy, we have measured the Hall resistance in which the relaxation rates cancel out in the first approximation, allowing in this way the estimation of the x dependence of the effective number of charge carriers.

The Hall resistivity of $Ru_{0.8}Sn_{0.2}Sr_2GdCu_2O_8$ as a function of magnetic field is shown in Fig. 8(a), for two temperatures below T_m, and compared to the results of the undoped sample.[16] A nonlinear increase in the Hall resistivity, which is the combination of the ordinary and extraordinary Hall contributions, and is a characteristic of magnetic metals, is observed at low fields. At high applied fields, a linear increase dominates, representing the ordinary Hall contribution only. The magnitude of the extraordinary contribution is smaller than that in the undoped sample [dotted line in Fig. 8(a)].

The average values of the Hall coefficient $R_H = d\rho_{xy}/d(\mu_0 H)$ are further plotted in Fig. 8(b) for low and high fields. Both, the low- and high-field slopes are smaller than for the pure compound. In particular, the absolute value of the ordinary R_H is roughly 30% smaller than in the pure compound, indicating a substantial increase in the effective number of charge carriers with Sn doping. Before discussing these data in more detail (Sec. IV B), it is useful to recall the prediction for R_H of the single-component free-hole model with the carrier concentration $n_{Cu}=2p/V_0$, which is found to explain the low-temperature Hall measurements in the well understood $La_{2-x}Sr_xCuO_4$ in the wide doping range $0.02 \leq p \leq 0.25$ (Ref. 22). With $V_0 \approx 170.5$ Å^3 being the primitive

cell volume of Ru1212Gd, the result is $R_H = 1.065 \cdot 10^{-9}/(2p)$ m^3/C. The measured high-field Hall coefficients indicated in Fig. 8(b) lead to $p=0.05$, 0.07 and 0.03 for the pure, Sn-doped and La-doped samples, respectively.

IV. DISCUSSION OF TRANSPORT COEFFICIENTS

In the following, we shall first show that the main changes in the present zero-field resistivity data, and in the (high-field) ordinary Hall coefficient data with Sn doping (which amounts to several tens of percent according to the inset of Fig. 6(a) and Fig. 8), can be explained by using a single-component model for the conductivity tensor (Sec. IV A), at variance with the experimental results reported in Ref. 2 which have been found to require the two-component model, with the charge carriers in the RuO_2 layers almost completely delocalized (notice in this respect a quite large ratio $\sigma_{Ru}/\sigma_{cu} \approx 0.5$ in Fig. 1 of Ref. 2, estimated from the thermopower data at $T<100$ K).

Within the present single-component model, only CuO_2 layers contribute to the observed conductivity, while the contributions of the RuO_2 layers to the total conductivity are small for the external magnetic fields absent and can be safely neglected in the first step.

Then, we shall argue, in subsection IV B, that this single-component model fails to account for the observed contribution to the magnetoresistivity (changes of the order of a few percent in Fig. 6), and the (low-field) Hall coefficient. Consequently, in order to successfully explain all our experimental observations, we have to go beyond the single-component model and take into account a presumably small number of itinerant electrons in the RuO_2 layers with a presumably strong coupling to the magnetic moments of the Ru ions.

When comparing two two-band models (the present one and that of Ref. 2), one is left to answer two questions which are fundamental to the quantitative understanding of the physics of the ruthenate-cuprates: first, to which extent the charge carriers in the RuO_2 layers are delocalized, and, second, the relative magnitude of the interactions between the Ru magnetic subsystem and the itinerant charge carriers in the CuO_2 layers and in the RuO_2 layers. In this context, the motivation for the two-step analysis of our data comes from the results of the zero-field NMR (NQR) experiments in the pure Ru1212Gd (Refs. 14 and 15) and the related band structure calculations.[23] The number of electrons in RuO_2 layers is equal to the number of holes doped into the CuO_2 plane. Naively, Ru^{4+} ion can be visualized as a composition of Ru^{5+} ion and one extra electron. In this picture, the basic question is as to which extent this extra electron is localized to the parent Ru^{5+} ion. In Ru-NQR experiments, two well-distinguished signals are found, corresponding to Ru^{5+} with the spin state $S=3/2$ and Ru^{4+} with the spin state $S=1$. These results suggest that most of the electrons are localized (leading to Ru^{4+} with the spin state $S=1$), which means that the number of itinerant (delocalized) electrons in the RuO_2 layers is small. In NQR, it is also found that the magnetic order in the RuO_2 layers coexists with the SC order in the CuO_2 planes down to $T=1.4$ K. Finally, the NQR frequency $\nu_Q^{63} \approx 30$ MHz measured on ^{63}Cu nuclei,[15,24] which is close to ν_Q^{63} measured in the underdoped $YBa_2Cu_3O_{6+x}$ compounds,[25] puts Ru1212*R* systems into the high-T_c superconductors with an intermediate copper-oxygen hybridization and, consequently, an intermediate value of T_c.[26]

The band structure calculations,[23] on the other hand, suggest the itinerant character of electrons in the RuO_2 layers, rather than the localized character, but all other conclusions of Ref. 23 are consistent with the NQR observations. Namely, there are three bands crossing E_F, the first two are related to two CuO_2 layers, while the third one is related to the RuO_2 layer. The magnetic ordering and the calculated magnitude of the magnetic moments of Ru ions are also consistent with the local magnetic fields measured by NQR.[14,15] Particularly important is the observation that two CuO_2 bands are not influenced significantly by the magnetism of the RuO_2 layers. Namely, the Cu $d_{x^2-y^2}$ states and the Ru d_{xy} states, which participate in three conduction bands, hybridize, respectively, with the p_z and $p_{x(y)}$ apex oxygen states, which are mutually orthogonal. The direct magnetic coupling (via apex oxygens only) between the charge carriers in these two subsystems thus vanishes for symmetry reasons.

In the present analysis, we neglect the presumably small coupling of the charge carriers (holes) in the CuO_2 layers to the Ru magnetic subsystem, and take that the effective concentration of these holes n_{Cu} is proportional to p ($n_{Cu} \approx 2p/V_0$) rather than to $1+p$. The latter proportionality is a consequence of the pseudogap formation due to the AFM fluctuation in the CuO_2 planes (see for example Ref. 27). Thus, n_{Cu} nearly measures the hole concentration in the CuO_2 bands with respect to the half-filling. The effective concentration of itinerant electrons in the RuO_2 layers n_{Ru} is assumed to be small in comparison to the value $2p/V_0$ characterizing the completely delocalized case, but, importantly, they are strongly coupled to the magnetic subsystem.

A. Resistivity and ordinary Hall coefficient

In the presence of the magnetic background of Ru^{5+}/Ru^{4+} ions and external magnetic fields, the conductivity tensor in question is given by[28]

$$\sigma_{xx} = \sigma_{yy} = \frac{e^2}{m}(\tau_{Cu}\tilde{n}_{xx}^{Cu} + \tau_{Ru}\tilde{n}_{xx}^{Ru}),$$

$$\sigma_{xy} = -\sigma_{yx} = \frac{e^2}{m}\omega_0(\tau_{Cu}^2\tilde{n}_{xy}^{Cu} + \tau_{Ru}^2\tilde{n}_{xy}^{Ru}) + \sigma_{xy}^{ex}. \quad (1)$$

The first term in the off-diagonal component σ_{xy} comes from the Lorentz force and is proportional to H (ω_0 is the cyclotron frequency). The second term, σ_{xy}^{ex}, includes all extraordinary contributions and is proportional to the magnetization of the Ru lattice, which means that the dependence on H is given in terms of the Brillouin function $B_S(g\mu_0\beta SH)$. According to Ref. 23, the contributions of two bands in Eq. (1) can be regarded as decoupled (i.e., the hybridization between the CuO_2 and RuO_2 bands is negligible). The structure of the effective numbers $\tilde{n}_{\alpha\beta}^i$, i=Cu, Ru and $\alpha,\beta=x,y$, for this case is given in the Appendix. For weak magnetic fields, for example, we obtain $\tilde{n}_{xx}^{Cu} \approx \tilde{n}_{xy}^{Cu} \approx n_{Cu}$ and $\tilde{n}_{xx}^{Ru} \approx -\tilde{n}_{xy}^{Ru} \approx n_{Ru}$, with

n_{Cu} and n_{Ru} defined above. τ_{Cu} and τ_{Ru} are, respectively, the relaxation times of holes and electrons averaged over two spin projections. For weak magnetic fields, it is reasonable to assume that not only $\tilde{n}^{Ru}_{\alpha\beta}$ is small, when compared to $\tilde{n}^{Cu}_{\alpha\beta}$, but also the relaxation rate in the RuO_2 layers $1/\tau_{Ru}$ is much larger than $1/\tau_{Cu}$, due to the presence of magnetic ions and the substitutional impurities in the RuO_2 layers. Thus, $\sigma^{Cu}_{\alpha\beta} \gg \sigma^{Ru}_{\alpha\beta}$ for $H=0$. But, as mentioned above, the main effects in the magnetoresistivity are expected to come from the field dependence of σ^{Ru}_{xx} [labeled hereafter by $\delta\sigma^{Ru}_{xx} = (e^2/m)\delta\tau_{Ru}\tilde{n}^{Ru}_{xx}$].

For weak magnetic fields, the general expressions for the Hall resistivity and magnetoresistivity

$$\rho_{xy} = \frac{\sigma_{xy}}{\sigma_{xx}\sigma_{yy} + \sigma^2_{xy}},$$

$$\rho_{xx} = \frac{\sigma_{xx}}{\sigma_{xx}\sigma_{yy} + \sigma^2_{xy}}, \tag{2}$$

lead to

$$\rho_{xy} \approx \frac{\sigma^{Cu}_{xy} + \sigma^{Ru}_{xy}}{(\sigma^{Cu}_{xx} + \sigma^{Ru}_{xx})^2},$$

$$\rho_{xx} \approx \frac{1}{\sigma^{Cu}_{xx} + \sigma^{Ru}_{xx}}, \tag{3}$$

i.e.,

$$\rho_{xy} \approx \frac{m}{e^2}\frac{\omega_0(\tau^2_{Cu}n_{Cu} - \tau^2_{Ru}n_{Ru}) + (m/e^2)\sigma^{ex;Ru}_{xy}}{(\tau_{Cu}n_{Cu} + \tau_{Ru}n_{Ru})^2},$$

$$\rho_{xx} \approx \frac{m}{e^2}\frac{1}{\tau_{Cu}n_{Cu} + \tau_{Ru}n_{Ru}}. \tag{4}$$

The Hall coefficient is given by $R_H = d\rho_{xy}/d(\mu_0 H)$. The anomalous contributions (the negative magnetoresistivity and the extraordinary Hall coefficient) are hidden here in $\delta\sigma^{Ru}_{xx}$ and $\sigma^{ex;Ru}_{xy}$, and we put $\delta\sigma^{Ru}_{xx} = \sigma^{ex;Ru}_{xy} = 0$ in the rest of this subsection.

In the Sn-doped samples, the replacement of any Ru atom by Sn introduces one extra hole in the system, which is redistributed between RuO_2 and CuO_2 layers. The part of the extra charge which remains in the RuO_2 layers decreases the effective number of itinerant electrons n_{Ru} ($\Delta n_{Ru} < 0$), thus increasing both the resistivity and Hall resistivity. One may say that it gives rise to the conversion of Ru^{4+} into Ru^{5+}. The part of the extra charge transferred into the CuO_2 layers increases the effective number n_{Cu} ($\Delta n_{Cu} > 0$). The experimentally determined decrease in the normal-state resistivity and the (high-field) Hall coefficient with the Sn doping (Figs. 6 and 8) shows that a substantial portion of the doped holes are indeed transferred to the CuO_2 layers and that the small changes in already small n_{Ru} can be neglected. This scenario is expected to hold for not too large number of Sn impurities ($x \leq 0.3$). Our results should be contrasted to the Sn doping study of McCrone *et al.* (Fig. 2 in Ref. 2), where the increase in resistivity and the Hall coefficient was observed for $x = 0.2$.

As mentioned above, the correlation between n_{Cu} and the superconducting critical temperature T_c is expected to be similar to the correlations found in the isostructural $YBa_2Cu_3O_{7-x}$ compounds. The main difference is that a very complicated role of the CuO chains in supporting superconductivity in the CuO_2 layers is played here by the magnetically ordered RuO_2 layers. Indeed, the dependence of T_c on the Sn doping x (shown in Fig. 3) is similar to the observation in the underdoped $YBa_2Cu_3O_{7-x}$ compounds (T_c is nearly constant in a wide range of x, $T_c \approx 60$ K in $YBa_2Cu_3O_{7-x}$).

A similar scenario also holds for other Ru1212*R* systems. For example, the replacement of Sr^{2+} by La^{3+} increases the total number of conduction electrons in the system. A substantial part of the doped electrons is transferred to the CuO_2 layers, reducing the effective number n_{Cu} below the critical value required for superconductivity, in agreement with experiments. In $RuSr_{1.9}La_{0.1}GdCu_2O_8$, the high-temperature resistivity and the high-field Hall resistivity are found to be increased by roughly 60%–70% with respect to the pure compound, and the superconductivity is completely suppressed.[17] The same effect of reducing the effective number n_{Cu} is obtained by the partial replacement of Ru ions by Nb.[2,4]

B. Magnetoresistivity

The magnetoresistivity data of Fig. 7 give us the indirect way to study the magnetic properties of the Ru lattice. In the model described above, we can write

$$\frac{\Delta\rho_{xx}}{\rho_{xx}(0)} = \frac{\rho_{xx}(H) - \rho_{xx}(0)}{\rho_{xx}(0)} \approx \frac{\sigma^{Ru}_{xx}(0)}{\sigma_{xx}(0)}\frac{\delta\rho^{Ru}_{xx}}{\rho^{Ru}_{xx}(0)}, \tag{5}$$

with $\sigma_{xx}(0)$ and $\sigma^{Ru}_{xx}(0)$ being, respectively, the zero-field total conductivity and the zero-field conductivity of the RuO_2 subsystem. The first factor is nearly proportional to $n_{Ru}/(n_{Cu}+n_{Ru})$ and represents an enhancement factor dependent on Sn doping. It grows with decreasing n_{Cu}, as can be easily seen from our data taken in three compounds: $Ru_{0.8}Sn_{0.2}Sr_2GdCu_2O_8$, $Ru_1Sr_2GdCu_2O_8$, and $Ru_{0.9}La_{0.1}Sr_2GdCu_2O_8$. The second factor in Eq. (5), $\delta\rho^{Ru}_{xx}/\rho^{Ru}_{xx}(0) \approx -\delta\sigma^{Ru}_{xx}/\sigma^{Ru}_{xx}(0)$, is the magnetoresistivity of the isolated RuO_2 subsystem, and it is expected to be similar to that of magnetic metals.[20,29,30] Precisely, the negative quadratic-in-field magnetoresistivity observed at temperatures well above T_m has to be contrasted to the magnetoresistivity of common high-T_c superconductors which is very small and positive.[31] This high-temperature behavior can be understood as a clear evidence of the exchange interaction between itinerant electrons in the RuO_2 layers and the localized Ru spins.[20] The AFM interactions between localized spins become important at low enough temperatures leading to the linear-in-field behavior with maximal slope at $T \approx T_m$ [Figs. 7(a)–7(c)]. We recall that exactly the same temperature evolution of the magnetoresistivity was found in Ref. 30 for small concentration of conduction electrons and low stability of the FM state of the localized spins. Hence, we believe that expression (5) includes all relevant processes in the magne-

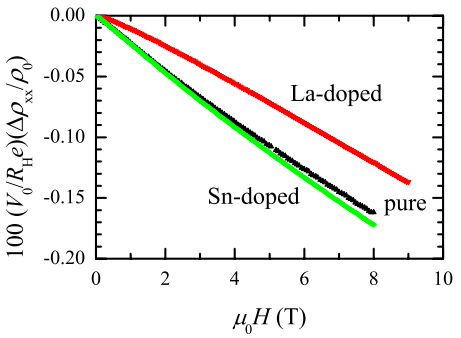

FIG. 9. (Color online) Field dependence of the quantity $V_0/(R_H e)[\Delta\rho_{xx}/\rho_{xx}(0)]$ for the pure ($RuSr_2GdCu_2O_8$), Sn-doped ($Ru_{0.8}Sn_{0.2}Sr_2GdCu_2O_8$) and La-doped ($RuSr_{1.9}La_{0.1}GdCu_2O_8$) samples at their respective magnetic ordering temperatures.

toresistivity of ruthenate-cuprates in the nonsuperconducting temperature range.

Taking into account that $\tau_{\mathrm{Ru}} n_{\mathrm{Ru}} \ll \tau_{\mathrm{Cu}} n_{\mathrm{Cu}}$, one can rewrite Eq. (5) in the form:

$$\frac{\delta\rho_{xx}^{\mathrm{Ru}}}{\rho_{xx}^{\mathrm{Ru}}(0)} \approx \frac{\tau_{\mathrm{Cu}} n_{\mathrm{Cu}}}{\tau_{\mathrm{Ru}} n_{\mathrm{Ru}}} \frac{\Delta\rho_{xx}}{\rho_{xx}(0)} \approx -\frac{\tau_{\mathrm{Cu}}}{\tau_{\mathrm{Ru}} V_0 n_{\mathrm{Ru}}} \frac{V_0}{R_H e} \frac{\Delta\rho_{xx}}{\rho_{xx}(0)}, \quad (6)$$

where $\Delta\rho_{xx}=\rho_{xx}(H)-\rho_{xx}(0)$. Figure 9 shows the field dependence of the quantity $V_0/(R_H e)[\Delta\rho_{xx}/\rho_{xx}(0)]$ for the three aforementioned samples at their respective magnetic ordering temperatures. If one assumes, based on the previous subsection, that $V_0 n_{\mathrm{Ru}} < 0.01$ and $\tau_{\mathrm{Ru}} < \tau_{\mathrm{Cu}}$, the magnetoconductivity of ruthenium layers is estimated to be several tens of percent at $\mu_0 H = 8$ T. The magnitude of this effect is comparable to the colossal magnetoresistivity of the manganite perovskites.[32]

V. CONCLUSIONS

In conclusion, a microwave study of Sn doping in Ru1212 samples has shown that magnetic ordering is strongly influenced by introduction of tin into RuO_2 layers, while the superconducting critical temperature remains practically unchanged.

The magnetic-field dependence of the microwave absorption has shown that the upper critical field in doped samples is increased, probably due to the increased disorder. However, in spite of increased disorder, the dc resistivity measurement in $Ru_{0.8}Sn_{0.2}Sr_2GdCu_2O_8$ is lower than in the respective pure compound. We conclude that it is due to the increased number of holes in the CuO_2 layers. This conclusion is also confirmed by Hall resistivity measurements presented in this paper.

In $Ru_{0.8}Sn_{0.2}Sr_2GdCu_2O_8$ magnetoresistivity develops from quadratic-in-field behavior (characteristic of uncorrelated magnetic impurities) at high temperatures to linear-in-field behavior close to $T_m \approx 76$ K, indicating significant correlations between magnetic Ru ions. Below T_m, a small positive component of magnetoresistivity, related to the AFM ordering of the RuO_2 lattice, is superimposed to the negative linear magnetoresistivity. As the temperature is lowered below 53 K, the field-induced ferromagnetic order seems to prevail. At the onset of superconductivity ($\approx$48 K) both positive superconducting and negative ferromagnetic contributions to the same magnetoresistivity curve occur.

We have shown that the single-component model for the conductivity tensor suffices to explain the variation of the normal-state resistivity and the high-field Hall coefficient with doping. The main conductivity channel is through CuO_2 layers and the various dopings simply change the number of conducting holes in these layers. However, the low-field Hall resistivity and the magnetoresistivity provide evidence that there is a small conduction in magnetically ordered RuO_2 layers. Quantitative analysis of the observed negative magnetoresistance leads to a quite remarkable conclusion that a small number of delocalized electrons displays a colossal magnetoresistance.

ACKNOWLEDGMENTS

We acknowledge funding support from the Croatian Ministry of Science, Education and Sports (projects no. 119-1191458-1022 "Microwave Investigations of New Materials", no. 119-1191458-0512 "Low-dimensional strongly correlated conducting systems" and no. 119-1191458-1023 "Systems with spatial and dimensional constraints: correlations and spin effects"), the New Zealand Marsden Fund, the New Zealand Foundation for Research Science and Technology, and the Alexander von Humboldt Foundation.

APPENDIX: CONDUCTIVITY TENSOR

In the multiband models with the interband hybridization negligible (Ru1212*R* systems are the example), the elements of the conductivity tensor are given by the sum of the intraband terms $\sigma_{\alpha\beta}=\Sigma_i \sigma_{\alpha\beta}^i$ (i=Cu, Ru in the present case). The presence of magnetic background and external magnetic fields makes, in the first place, the relaxation rates of conduction electrons $\Gamma_{i\sigma}(\mathbf{k})=1/\tau_{i\sigma}(\mathbf{k})$ depend on spin, and also introduces the extraordinary contributions to the off-diagonal elements of the conductivity tensor $\sigma_{xy}^{\mathrm{ex}:i}$, as discussed in the main text. In the first approximation (the case of noninteracting magnetic impurities[20]) we can write $\Gamma_{i\sigma}(\mathbf{k}) \approx \Gamma_i \pm \alpha_i M_z$, where α_i is a constant and M_z is the total magnetization of the RuO_2 layer. Thus, in the Ru1212*R* systems, at temperatures well above T_m, we have $\sigma_{xx}^i=\sigma_{yy}^i=(e^2/m)\tau_i\tilde{n}_{xx}^i$ and $\sigma_{xy}^i=-\sigma_{yx}^i=(e^2/m)\omega_0\tau_i^2\tilde{n}_{xy}^i+\sigma_{xy}^{\mathrm{ex}:i}$, with $\tau_i\tilde{n}_{xx}^i$ and $\tau_i^2\tilde{n}_{xy}^i$ given by[28]

$$\tau_i\tilde{n}_{xx}^i \approx \frac{1}{V}\sum_{\mathbf{k}\sigma} \frac{m[v_x^i(\mathbf{k})]^2\tau_{i\sigma}(\mathbf{k})}{1+\tau_{i\sigma}^2(\mathbf{k})\omega_{i0}^2(\mathbf{k})}(-)\frac{\partial f_{i\sigma}(\mathbf{k})}{\partial\varepsilon_{i\sigma}(\mathbf{k})},$$

$$\tau_i^2\tilde{n}_{xy}^i \approx \frac{1}{V}\sum_{\mathbf{k}\sigma} \frac{mv_x^i(\mathbf{k})[v_x^i(\mathbf{k})\gamma_{yy}^j(\mathbf{k})-v_y^i(\mathbf{k})\gamma_{xy}^j(\mathbf{k})]}{1+\tau_{i\sigma}^2(\mathbf{k})\omega_{i0}^2(\mathbf{k})} \times \tau_{i\sigma}^2(\mathbf{k})\frac{\partial f_{i\sigma}(\mathbf{k})}{\partial\varepsilon_{i\sigma}(\mathbf{k})}. \quad (A1)$$

$v_x^i(\mathbf{k})$ is the electron group velocity, $\omega_{i0}^2(\mathbf{k})=\gamma_{xx}^j(\mathbf{k})\gamma_{yy}^j(\mathbf{k})\omega_0^2$, and $\gamma_{\alpha\beta}^j(\mathbf{k})=(m/\hbar^2)\partial^2\varepsilon_{i\sigma}(\mathbf{k})/\partial k_\alpha \partial k_\beta$ are the elements of the inverse effective-mass tensor.

For weak magnetic fields, the relaxation times independent of $\mathbf{k}$, and $\gamma^j_{\alpha\beta}(\mathbf{k}) \propto \delta_{\alpha\beta}$, we obtain the textbook expressions

$$n^i_{xx} \approx \frac{1}{V}\sum_{\mathbf{k}\sigma} m[v^i_x(\mathbf{k})]^2(-)\frac{\partial f_{i\sigma}(\mathbf{k})}{\partial \varepsilon_{i\sigma}(\mathbf{k})},$$

$$n^i_{xy} \approx \frac{1}{V}\sum_{\mathbf{k}\sigma} m[v^i_x(\mathbf{k})]^2\gamma^j_{yy}(\mathbf{k})\frac{\partial f_{i\sigma}(\mathbf{k})}{\partial \varepsilon_{i\sigma}(\mathbf{k})}, \tag{A2}$$

which we use in the discussion in the main text. The effects of the AFM correlations on the effective numbers $n^{\mathrm{Cu}}_{\alpha\beta}$ are included here through the dependence of $\varepsilon_{\mathrm{Cu}}(\mathbf{k})$, $v^{\mathrm{Cu}}_x(\mathbf{k})$, and $\gamma^{\mathrm{Cu}}_{\alpha\beta}(\mathbf{k})$ on the AFM (pseudo)gap scale, as explained in detail in Sec. VIA and Fig. 12 of Ref. 27. The main result of this analysis is that the effective numbers $n^{\mathrm{Cu}}_{\alpha\beta}$ are proportional to the number of holes p measured with respect to the half-filled Cu band, rather than to the total number of holes in the Cu band $1+p$.

If magnetic fields are weak and the exchange interaction between the conduction holes and localized Ru spins is negligible, the field dependence in the denominators in Eq. (A1) can again be neglected, and the sum over spin projections gives for the averaged relaxation times of itinerant electrons the expression $\Sigma_\sigma \tau_{\mathrm{Ru}\sigma}(\mathbf{k}) \approx 2\Gamma^0_{\mathrm{Ru}}/[(\Gamma^0_{\mathrm{Ru}})^2 - \alpha^2_{\mathrm{Ru}}(M_z)^2]$, resulting in $\delta\sigma^{\mathrm{Ru}}_{xx} \propto H^2$.[20] According to Eq. (5), this also leads to the total magnetoresistivity which is negative and quadratic-in-field. The effects of interactions between localized spins on the conductivity tensor at different temperatures are expected to be similar to that found in Ref. 30.

[1] T. Nachtrab, C. Bernhard, L. Chengtian, D. Koelle, and R. Kleiner, C. R. Phys. **7**, 68 (2006).
[2] J. E. McCrone, J. L. Tallon, J. R. Cooper, A. C. MacLaughlin, J. P. Attfield, and C. Bernhard, Phys. Rev. B **68**, 064514 (2003).
[3] P. W. Klamut, B. Dabrowski, S. Kolesnik, M. Maxwell, and J. Mais, Phys. Rev. B **63**, 224512 (2001).
[4] A. C. Mclaughlin, V. Janowitz, J. A. McAllister, and J. P. Attfield, J. Mater. Chem. **11**, 173 (2001).
[5] G. V. M. Williams, H. K. Lee, and S. Krämer, Phys. Rev. B **67**, 104514 (2003).
[6] A. Hassen and P. Mandal, Supercond. Sci. Technol. **19**, 902 (2006).
[7] A. C. McLaughlin and J. P. Attfield, Phys. Rev. B **60**, 14605 (1999).
[8] S. Malo, K. Donggeun, J. T. Rijssenbeek, A. Maignan, D. Pelloquin, V. P. Dravid, and K. R. Poeppelmeier, Int. J. Inorg. Mater. **2**, 601 (2000).
[9] A. Hassen, J. Hemberger, A. Loidl, and A. Krimmel, Physica C **400**, 71 (2003).
[10] Y. Yamada, H. Hamada, M. Shimada, S. Kubo, and A. Matsushita, J. Magn. Magn. Mater. **272-276**, e173 (2004).
[11] M. Steiger, C. Kongmark, F. Rueckert, L. Harding, and M. S. Torikachvili, Physica C **453**, 24 (2007).
[12] P. W. Klamut, B. Dabrowski, J. Mais, and M. Maxwell, Physica C **350**, 24 (2001).
[13] T. P. Papageorgiou, E. Casini, Y. Skourski, T. Herrmannsdörfer, J. Freudenberger, H. F. Braun, and J. Wosnitza, Phys. Rev. B **75**, 104513 (2007).
[14] Y. Tokunaga, H. Kotegawa, K. Ishida, Y. Kitaoka, H. Takagiwa, and J. Akimitsu, Phys. Rev. Lett. **86**, 5767 (2001).
[15] K. I. Kumagai, S. Takada, and Y. Furukawa, Phys. Rev. B **63**, 180509(R) (2001).
[16] M. Požek, A. Dulčić, D. Paar, A. Hamzić, M. Basletić, E. Tafra, G. V. M. Williams, and S. Krämer, Phys. Rev. B **65**, 174514 (2002).
[17] M. Požek, A. Dulčić, A. Hamzić, M. Basletić, E. Tafra, G. V. M. Williams, and S. Krämer, Eur. Phys. J. B **57**, 1 (2007).
[18] B. Nebendahl, D.-N. Peligrad, M. Požek, A. Dulčić, and M. Mehring, Rev. Sci. Instrum. **72**, 1876 (2001).
[19] D. Janjušević, M. S. Grbić, M. Požek, A. Dulčić, D. Paar, B. Nebendahl, and T. Wagner, Phys. Rev. B **74**, 104501 (2006).
[20] K. Yosida, Phys. Rev. **107**, 396 (1957).
[21] T. He, Q. Huang, and R. J. Cava, Phys. Rev. B **63**, 024402 (2000).
[22] Y. Ando, Y. Kurita, S. Komiya, S. Ono, and K. Segawa, Phys. Rev. Lett. **92**, 197001 (2004).
[23] K. Nakamura, K. T. Park, A. J. Freeman, and J. D. Jorgensen, Phys. Rev. B **63**, 024507 (2000).
[24] S. Krämer and G. V. M. Williams, Physica C **377**, 282 (2002).
[25] H. Yasuoka, T. Imai, and T. Shimizu, in *Strong Correlations and Superconductivity*, Springer Series in Solid State Sciences Vol. 89 (Springer, Berlin, 1989), p. 254.
[26] I. Kupčić, S. Barišić, and E. Tutiš, Phys. Rev. B **57**, 8590 (1998).
[27] I. Kupčić and S. Barišić, Phys. Rev. B **75**, 094508 (2007).
[28] J. M. Ziman, *Electrons and Phonons* (Oxford University Press, London, 1972).
[29] A. Fert, R. Asomoza, D. H. Sanchez, D. Spanjaard, and A. Friederich, Phys. Rev. B **16**, 5040 (1977).
[30] M. Kataoka, Phys. Rev. B **63**, 134435 (2001).
[31] J. M. Harris, Y. F. Yan, P. Matl, N. P. Ong, P. W. Anderson, T. Kimura, and K. Kitazawa, Phys. Rev. Lett. **75**, 1391 (1995).
[32] J. Fontcuberta, B. Martínez, A. Seffar, S. Piñol, J. L. García-Muñoz, and X. Obradors, Phys. Rev. Lett. **76**, 1122 (1996).